

# Determination of the ionization energy and the electron affinity of organic molecular crystals from first-principles: dependence on the molecular orientation at the surface

Susumu Yanagisawa<sup>1,\*</sup>

<sup>1</sup>*Department of Physics and Earth Sciences, Faculty of Science,  
University of the Ryukyus, 1 Senbaru, Nishihara, Okinawa 903-0213, Japan*

(Dated: November 27, 2019)

I demonstrate that the ionization energy (IE) and the electron affinity (EA) of organic molecular crystals can be predicted from first-principles. Here, I describe the induced electronic polarization and the electrostatic effects upon crystalline IE and EA. I also demonstrate that the electronic polarization mainly originates from the screened coulomb interaction inside the crystalline bulk phase, and that the electrostatic contribution to IE and EA crucially depends on the orientation of the molecule at the surface. The former is well described by the *GW* approximation, while the latter is reasonably estimated by the difference in frontier orbital energy between the gas phase and the surface at the level of a generalized gradient approximation to the density functional theory. The present methodology enables to demonstrate the impact of the electrostatic effect upon the energy level of the injected charge at a multi-monolayer surface of an organic semiconductor thin film.

## I. INTRODUCTION

Ionization energy (IE) and electron affinity (EA) are fundamental physico-chemical quantities of organic semiconductors, and understanding the factors that determine the energy levels is of primary importance to the research and development of the organic electronics materials such as those of organic light-emitting diodes (OLEDs), organic field-effect transistors (OFETs), and organic photovoltaics (OPVs), dominating energy barrier for injection of a charge carrier (hole and electron).<sup>1,2</sup> The fundamental gap is the difference between IE and EA, thus also affecting the conductive properties.

IE and EA are measured with direct photoemission and inverse photoemission techniques, respectively. Notice here that the energy of the hole or electron injected into the sample is measured, i.e., IE (EA) is the magnitude of the energy difference between the neutral  $N$ -electron and the positively-(negatively-)charged  $N-1$  ( $N+1$ )-electron systems. Thus, the measured IE and EA implies many-body interaction between the injected charge and the surrounding polarization clouds inside the organic solids which screen the injected charge. A complex of the injected charge and the surrounding dynamically induced polarization clouds are referred to as quasiparticles, which are theoretically well-described with the self-energy determined by the many-body perturbation theory within the *GW* approximation.<sup>3,4</sup>

While the *GW* method describes well the electronic polarization upon the injected charge, the numerical details and the program codes of the *GW* approximation have been developed mainly for three-dimensional periodic or bulk systems, since the perturbation upon the free electron gas was implied. For lower dimension systems such as surfaces and interfaces, it is necessary to eliminate the artificial long-range screened coulomb interaction between the periodic replicas that are arranged along the non-periodic direction, with the technique such as the coulomb cutoff.<sup>5,6</sup> However, at present, only a few works

reported the *GW*-level quasiparticle energy at surfaces or interfaces comprised of a few organic monolayers,<sup>7-10</sup> possibly because of the computational cost required and the difficulty in numerical convergence, despite the academic and technical interest in low-dimensional systems relevant to realistic device structures.

Theoretical predication of IE and EA of organic semiconductors from first-principles was demonstrated by modeling an organic molecule in a solid with the polarizable continuum model (PCM)<sup>11</sup> or the quantum mechanics/molecular mechanics (QM/MM)<sup>12-15</sup> approach. The methodology demonstrated reasonable accuracy in estimating IE and EA of organic semiconductors with the density functional theory (DFT).<sup>16-19</sup> For more accurate treatment, the *GW* approximation was employed. Combination of the QM/MM approach and the implementation of the *GW* approximation with a localized basis set<sup>20</sup> enabled theoretical prediction of IE and EA of an organic molecule embedded inside the bulk or at the surface of the organic semiconductor.<sup>21,22</sup> The result was found to be more quantitative than the previous approaches. The screening of the coulomb potential slightly smaller at the surface than at the bulk was also demonstrated, because the method allows to describe the surface morphology.

Given that an experimental measurement of a few organic monolayers on a substrate such as silica and graphite is available, it is of importance to investigate the electronic structure of an organic film of a few monolayer thickness with a reliable theoretical method such as the *GW* approximation. For such purposes, a periodic slab model approach is useful. To avoid the computationally demanding periodic slab calculation with *GW*, the electrostatic potential in a periodic slab was described within DFT-GGA,<sup>23</sup> which was aligned to that in a bulk system.<sup>24</sup> In the bulk system, the electronic polarization upon the injected charge was described within the *GW* approximation. The resulting IE and EA depending on the surface morphology was described well.

In this paper, with a combination of the *GW* approxi-

mation suitable in general to solid or bulk systems and a periodic slab approach at the DFT-GGA level, I investigated typical polymorphs of pentacene (PEN) and perfluoropentacene (PFP). They are known as ideal molecules for the purpose of distinguishing between the roles of electronic polarization and electrostatic contributions, with their same  $\pi$ -conjugated back bones and the opposite polarity of C-H and C-F bonds, thus resulting in nearly equal molecular polarizabilities, and principal components of the quadrupole moment of similar magnitude but opposite sign.<sup>25</sup>

I theoretically demonstrated that the IE and EA at the surface are dominated by the electronic polarization upon the injected charge induced by the surrounding polarization clouds, and the electrostatic energy crucially affected by the orientation of the molecule at the surface of the organic semiconductor. In other words, the electronic polarization and the electrostatic contributions dominantly constitute the polarization energy.<sup>26,27</sup> The electronic polarization is isotropic and short-ranged, dominated by the electronic property of the organic semiconductor bulk. On the other hand, the origin of the impact of the electrostatic potential was proposed to be the interaction between the charge and the permanent quadrupole moment of the constituent molecules.<sup>28</sup> It is shown that the electronic polarization effect is accurately estimated with the *GW* approximation, and that the electrostatic contribution dominated by the molecular orientation at the surface of the organic semiconductor can be estimated reasonably accurately with DFT-GGA.

The same methodology was already successfully applied to a monolayer of 6,13-pentacenequinone, in comparison to the experimental measurement,<sup>29</sup> and a preliminary result of the present work was demonstrated elsewhere.<sup>30</sup> The central point of this work, i.e., the roles of the electronic polarization and the electrostatic contributions in the polarization energy, clarified by investigating both PEN and PFP, was not deeply discussed in the previous work.<sup>30</sup>

## II. BACKGROUND AND DETAIL OF THE THEORETICAL METHOD

### A. IE and EA of an organic solid: roles of electronic polarization and electrostatic energies

Since the intermolecular interaction is usually smaller than the intramolecular one by an order of magnitude or more, the energy level of an organic solid can be well approximated by the electronic level of an isolated molecule perturbed by the weak interaction induced by the classical or quantum mechanical effects.<sup>31-33</sup> It was proposed<sup>26,29</sup> that IE ( $I_s$ ) and EA ( $A_s$ ) in a solid are defined as

$$I_s = I_g - P^+ - \Delta^+, A_s = A_g + P^- + \Delta^-, \quad (1)$$

where the subscripts g and s denote a gas phase and a solid phase, respectively. The effect of bandwidths of the highest-occupied molecular orbital (HOMO)- and the lowest-unoccupied molecular orbital (LUMO)-derived bands,  $\Delta^+$  and  $\Delta^-$ , is taken into account.

The polarization energies for positive  $P^+$  and negative  $P^-$  charges consist of the electronic polarization energy  $E_p$  and the electrostatic energy  $S$ ,

$$P^+ = E_p^+ + S^+, P^- = E_p^- + S^-. \quad (2)$$

The electronic polarization energy  $E_p$ , also referred to as the dynamical interaction,<sup>27</sup> is an induced effect to minimize the total energy, and is approximated by the charge-induced dipole interaction. The  $S$ , on the contrary, is the electrostatic interaction between the injected excess charge and the charge distributed over the constituent neutral molecules of the organic solid. Both the terms originate from the classical electrostatic interaction, while the  $\Delta$  corresponds to the quantum mechanical effect. The  $E_p$  is short-ranged and isotropic, and its magnitude is almost independent of the organic materials, ranging from 1 to 2 eV.<sup>34</sup> On the other hand, the  $S$  has been proposed to be the origin of the orientation dependence of  $I_s$  and  $A_s$  in molecular films.<sup>35</sup> The experimentally observed molecular orientation dependence of the ionization energy has been proposed to originate from the electrostatic potential generated by the permanent quadrupole moment of molecules, based on the theoretical studies.<sup>26,28,36</sup> In addition to the orientation dependence of the energy level for standing and lying orientations, the dependence on the molecular orientations with different orientation angles was confirmed by the measurement of  $I_s$  and  $A_s$  of the organic thin film by carefully tuning the molecular orientation angle on the same substrate.<sup>29</sup>

In this work, considering the nature of the electronic polarization and the electrostatic contribution to the polarization energy  $P$ , I estimated the  $E_p$  for the organic semiconductor bulk with the *GW* approximation, and the  $S$  was obtained with the periodic slab model of the organic semiconductor surface at the DFT-GGA level of theory. Notice that the interaction between  $E_p$  and  $S$  was proposed to be insignificant,<sup>28</sup> and, I therefore neglected the cross term between  $E_p$  and  $S$ .

### B. Details of the theoretical calculation

#### 1. Optimization of the internal geometries of PEN and PFP crystals

The geometrical configurations of the organic semiconductor bulk (Fig. 1) was determined with the STATE program code,<sup>37</sup> with the lattice constants fixed to the experimental values. For the crystal structure and the lattice constants, two typical polymorphs were considered: single crystal<sup>38</sup> and thin film<sup>39</sup> phases of PEN, fabricated on  $\text{SiO}_2$ <sup>40</sup> and graphene<sup>41</sup> substrates, respectively,

and, herringbone<sup>42</sup> and  $\pi$ -stacking motifs<sup>43</sup> for PFP, that were reported to grow on the SiO<sub>2</sub> and graphene, respectively. For optimization of the atomic configurations in the unit cells with their experimental lattice vectors fixed,<sup>38,39,42,43</sup> I used the dispersion correction to GGA-PBE<sup>23</sup> exchange-correlation denoted by DFT-D2,<sup>44</sup> so that the intermolecular van der Waals forces were taken into account. I used the *ab initio* norm-conserving pseudopotentials to describe the electron-ion interaction,<sup>45</sup> and the wave function was expanded by using a plane-wave basis set with the cutoff energy of 72 (100) Ry for PEN (PFP) crystals. The structures were allowed to relax until all the forces upon the atoms dropped below 0.06 nN. A  $\mathbf{k}$ -point mesh of  $4 \times 3 \times 2$  was used for PEN crystals, and that of  $2 \times 6 \times 2$  ( $2 \times 4 \times 4$ ) was used for the herringbone ( $\pi$ -stacking) motif of PFP.

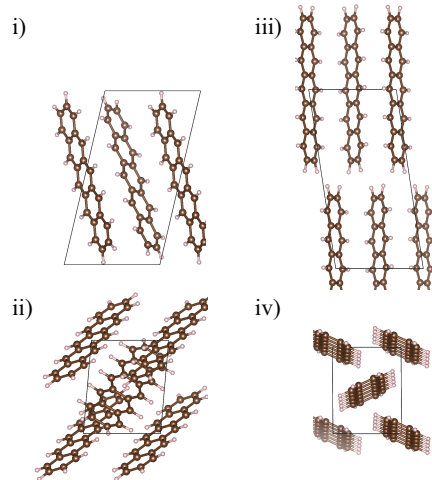
## 2. Calculation of the electronic polarization $E_p$ to the polarization energy $P$

For the optimized crystal geometries, I estimated the  $E_p^+$  and  $E_p^-$  upon the excess hole and electron, respectively, based on the quasiparticle self-energy within the *GW* approximation.<sup>3,4,46</sup> Here, the fundamental band gaps of the PEN and PFP crystals were calculated. I used the modified version of the *GW* space-time code,<sup>47-49</sup> which enables highly parallelized calculations with thousands of CPU cores.

The perturbative *GW* ( $G_0W_0$ ) calculations were based on the norm-conserving pseudopotentials and plane-wave basis set. The starting wave functions were generated with the GGA-PBE functional using the STATE code. To calculate the correlation part of the *GW* self-energy, I evaluated the full frequency dependence of the dielectric function numerically. On the imaginary frequency/time axis, the relevant quantities such as polarizability, dielectric function, screened coulomb potential, and self-energy have smoothly decaying tails, which are fitted to simple model functions. The remaining frequency/time region around zero is treated numerically. The matrix elements of the correlation self-energy on the imaginary time axis are fitted to the model function, followed by the fast Fourier transform to those on the imaginary frequency axis, and then analytic continuation onto the real energy axis.<sup>48</sup>

In addition to the one-shot  $G_0W_0$  calculation, I performed the eigenvalue-only self-consistent *GW* calculations (ev*GW*),<sup>50,51</sup> so that the starting point dependence<sup>20,52-56</sup> of the  $G_0W_0$  calculations was removed. In the ev*GW* calculations, only the diagonal part of the self-energy was considered, and only the eigenvalues were updated in constructing the Green's function and the screened Coulomb potential while retaining the wave functions unchanged, under the assumption that the starting DFT wave functions are close to the true quasiparticle ones.<sup>46,57</sup> In this study, the quasiparticle energies of up to the second lowest unoccupied band were

### (a) Pentacene



### (b) Perfluoropentacene

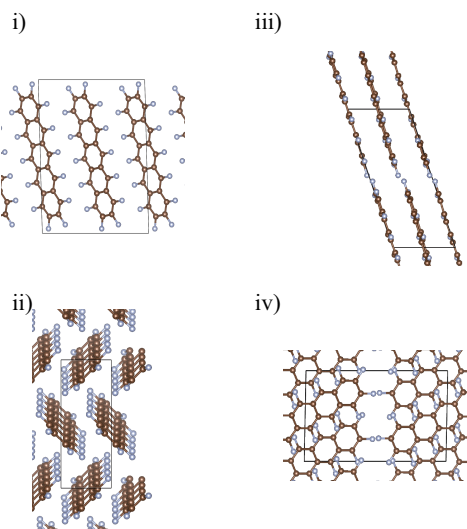


FIG. 1. Overviews of the crystal structures of (a) pentacene and (b) perfluoropentacene polymorphs. (a)-i, ii) and -iii, iv) display the structures of the unit cells of PEN single crystal and thin film phase, respectively, and (b)-i, ii) and -iii, iv) show those of the PFP herringbone and  $\pi$ -stack motifs, respectively. The solid lines display the shape of the unit cell, and two molecules are positioned at the corner and center of the unit cell. They are arranged in a herringbone-like fashion, except in the unit cell of PFP  $\pi$ -stack motif. The molecular planes are almost perpendicularly stacked along the PFP  $\pi$ -stacking direction.

updated, so that the energies of the bands up to those derived from the LUMO of the two molecules in the unit cell is updated appropriately. The energies of the higher bands outside the preset energy window were corrected by a scissors-like operation, that is, they were shifted rigidly by  $\Delta = E_{m\mathbf{k}} - \varepsilon_{m\mathbf{k}}^{\text{DFT}}$ , where  $E_{m\mathbf{k}}$ ,  $\varepsilon_{m\mathbf{k}}^{\text{DFT}}$  are respectively the quasiparticle energy and the DFT eigenvalue in the highest band  $m$  in the preset energy window (second

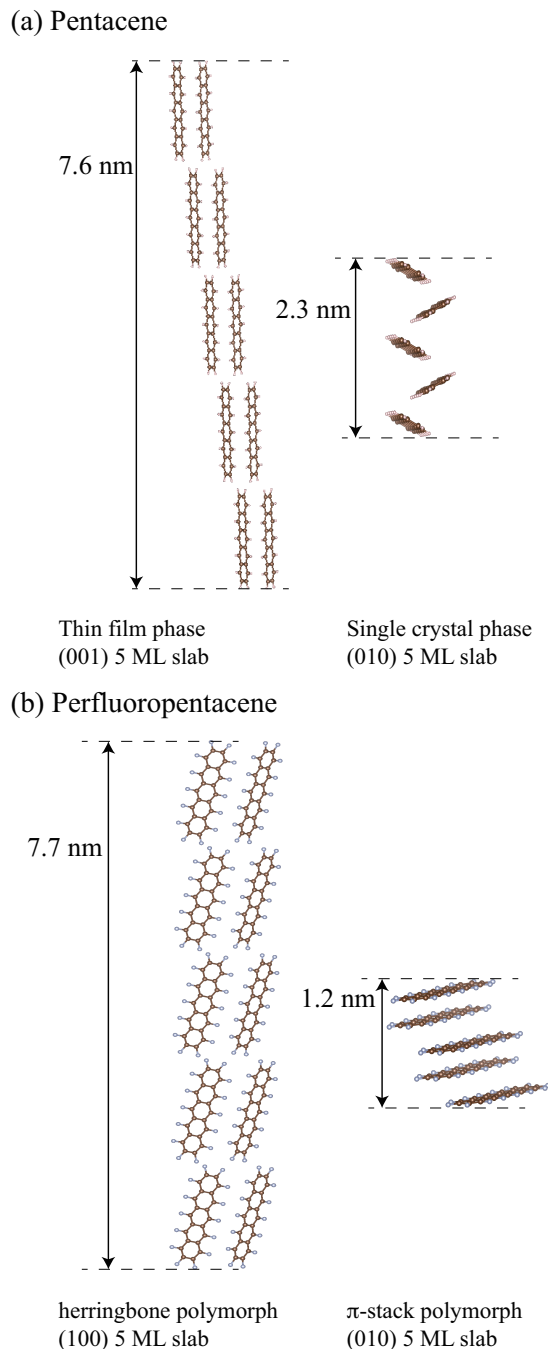


FIG. 2. Overviews of the slab geometry of (a) pentacene (PEN) and (b) perfluoropentacene (PFP) polymorphs. In (a) and (b), the left panels display the structures of the 5 ML (100) facets of PEN thin film and PFP herringbone polymorphs in the standing configuration, respectively. The right panels show the structures of the 5 ML slabs of the (010) facets of PEN single crystal and PFP  $\pi$ -stack polymorphs in the lying configuration, respectively. Their nominal thickness along the normal of the surface is also displayed.

lowest unoccupied band in the present study). I found that five or six iterations were necessary to converge the fundamental gap within 0.01 eV.

The calculated quasiparticle self-energy was averaged over the  $\mathbf{k}$ -points sampled in the Brillouin zone, so that the result corresponded to the experimentally measured fundamental gap, which in general represents the difference between the density-of-states (DOS) peaks of the highest-occupied and the lowest-unoccupied band energies. I used the same  $\mathbf{k}$ -point meshes as in the prior DFT-GGA calculation, and the plane-wave cutoffs of 40 Ry was used. The number of empty states used in the calculation of the Green's function was 5281 (PEN) and 6584 (PFP) bands, which encompass more than 200 eV above the center of the band gap. The convergence of the calculated band gap with respect to the number of empty states,  $\mathbf{k}$ -point sampling, and plane-wave cutoff is estimated to be within 0.05 eV.

The electronic polarization  $E_p$  was obtained as half the difference between the crystalline fundamental gap and that in a gas phase, assuming that  $E_p^+ = E_p^-$ . For the gas phase IE ( $I_g$ ) and EA ( $A_g$ ), I used the experimentally reported  $I_g$  for PEN of 6.589 eV<sup>58</sup> and PFP of 7.50 eV,<sup>59</sup> experimental  $A_g$  for PEN of 1.392 eV,<sup>26,60</sup> and theoretical  $A_g$  for PFP of 2.66 eV,<sup>61</sup> rather than calculating the *GW*-level gas-phase fundamental gap which requires self-consistency to improve the over-screening of the injected charge,<sup>53,62</sup> along with the coulomb cutoff technique<sup>5,6</sup> and use of a large supercell to avoid the artificial interaction between the periodic neighboring unit cells.

### 3. The electrostatic contributions $S^+$ and $S^-$

To describe the orientation dependence of the highest-occupied or the lowest-unoccupied level energies in a multi-layer slab, the difference in energy level between a five monolayer periodic slab (see Fig. 2) and an isolated gas-phase molecule was calculated at the DFT-GGA level of theory, after optimizing the geometries with DFT-D2. Here, I used the ultrasoft pseudopotentials,<sup>63</sup> with the plane-wave energy cutoff of 25 Ry and 400 Ry for wave functions and charge density, respectively, and the surface Brillouin zone was sampled with the in-plane  $\mathbf{k}$ -point mesh similar to the above-mentioned bulk crystal calculation.

The highest-occupied or lowest-unoccupied energy in a five monolayer slab was estimated by averaging the energies of the five or ten highest occupied- or unoccupied band energies over the surface Brillouin zone for the facets of PEN and PFP crystal surfaces, i.e. (010) and (001) surfaces for PEN single crystal<sup>38</sup> and thin film phases,<sup>39</sup> respectively, and (100) and (010) facets for PFP herringbone<sup>42</sup> and  $\pi$ -stacking<sup>43</sup> motifs, respectively. Associated with their molecular configurations in Fig. 2, the configuration at a (001) facet of PEN thin film and that at a (100) facet of PFP herringbone were referred to as

"standing" configuration, and the other configurations as "lying" configurations. The  $\mathbf{k}$ -averaged highest-occupied or lowest-unoccupied energies almost corresponds to the center of their DOS peak, and thus implicitly includes the quantum mechanical effect or the bandwidth effect  $\Delta^+/\Delta^-$  defined in Eq. 1. The highest-occupied (lowest-unoccupied) energies to be averaged ranged over 0.63 eV (0.66 eV) for PEN thin film (001), 0.45 eV (0.58 eV) for PEN single crystal (010), 0.62 eV (0.38 eV) for PFP herringbone (100), and 0.51 eV (0.33 eV) for PFP  $\pi$  stack (010), respectively, and they reasonably agreed with the bandwidths of the same materials calculated at the same level of theory.<sup>26,64</sup>

The electrostatic contribution in the polarization energy  $S^+$  or  $S^-$  (see Eq. 2) may be approximated by the difference in the highest-occupied or the lowest-unoccupied energy level between the multi-layer slab and an isolated molecule. The approximation may be valid because of the "nearsightedness" of the quantum mechanical effects, i.e., perturbation of the external potential at a region distant from a given location by a distance larger than a typical de Broglie wavelength has a small effect upon any static property of a many-particle system at that location.<sup>65,66</sup> In other words, a local chemical environment or intramolecular chemical interaction in a free-standing monolayer is similar to that in an isolated single molecule. On the other hand, the different electrostatic interactions in a monolayer and in a gas phase were demonstrated theoretically.<sup>66</sup>

Overall, with the theoretical  $S^+$  and  $S^-$ , and  $E_p$ , the  $I_s$  and  $A_s$  are theoretically determined according to Eqs. 1 and 2 (see also Fig. 3).

### III. RESULTS AND DISCUSSION

#### A. Theoretical fundamental band gap and Ionization energy $I_s$ and electron affinity $A_s$ of the organic crystals

Tables I and II display the calculated  $I_s$  and  $A_s$  at the surfaces of PEN and PFP, respectively, and the results are schematically displayed in Fig. 3. The theoretical  $I_s$  and  $A_s$  were in agreement with the experimental  $I_s$  measured with the direct photoemission technique<sup>43,67-75</sup> and  $A_s$  that were recently determined with the low-energy inversion photoemission spectroscopy (LEIPS) measurement.<sup>26</sup> The fundamental gap  $I_s - A_s$  estimated with the one-shot  $G_0W_0$  ranged from 2.2~2.5 eV, which were in general slightly smaller than the experimental values. When the partially self-consistent *evGW* was used, the fundamental gap increased by 0.6~0.7 eV, as a result of the diminished starting point dependence (the DFT-GGA-based band gap, used as a starting point, is severely underestimated compared to experiments<sup>76</sup>). They were in general overestimated by 0.4-0.6 eV compared to the experimental fundamental gaps, and they were in agreement with the theoretical bulk band gap ob-

tained with the embedded *GW* formalism<sup>22</sup> or other *GW* studies on bulk pentacene employing self-consistency similar to this work.<sup>24,76</sup> The agreement between the *GW* results and the experimental values might improve if more flexible self-consistency with updated one-particle wave functions was employed. Taking into account the decreasing polarization at the surface compared to the crystalline bulk, which was proposed to make the band gap larger by  $\approx 0.2$  eV,<sup>22</sup> but was not taken into account in this work, should also be considered. In terms of the calculated  $I_s$  and  $A_s$  in this work, the *evGW* resulted in increasing  $I_s$  and decreasing  $A_s$  by 0.3 eV, and, thus the overall mean absolute deviations (MADs) of  $G_0W_0$  and *evGW* from experiments are similar (MADs of 0.18 eV ( $G_0W_0$ ) and 0.27 eV (*evGW*)). At the moment, I would like to leave it a future work to improve the theoretical treatment. In the followings, I will focus on the dependence of the theoretical  $I_s$  and  $A_s$  on the molecular orientation at the surface.

#### B. Dependence of $I_s$ and $A_s$ on the surface molecular orientation

Notice that the trends of the theoretical  $I_s$  and  $A_s$  of PEN and PFP depending on the molecular orientation at the surface (see Figs. 2 and 3) are opposite. In case of PEN, the *standing* orientation at the (001) surface of the thin film phase gives smaller  $I_s$  and  $A_s$  (or higher energy levels of the injected charges) than those of the *lying* orientation at the (010) surface of the single crystal phase. On the other hand, for PFP, the *lying* orientation at the (010) facet of the  $\pi$ -stack motif results in lower binding energies of the injected charges than the *standing* orientation at (100) of the herringbone motif.

Given that the electronic polarization contribution  $E_p$  is similar in PEN and PFP (see Tables I and II), the different trend of the  $I_s$  and  $A_s$  depending on the facet of the motif originates from the different electrostatic contribution  $S^+$  and  $S^-$ . As discussed before, the different  $S^+$  and  $S^-$  for different facets of PEN and PFP, a neutral molecule with no molecular permanent dipole and their difference in polarity of C-H and C-F bonds, may be elucidated by the different quadrupole-charge interaction of the molecules.<sup>25,26,28</sup> The  $S^+$  and  $S^-$  with their similar magnitudes but opposite signs as found in this study are reasonable in that they originate from the electrostatic interaction of the injected charge with the surroundings.<sup>28</sup> The slight difference in magnitude between  $S^+$  and  $S^-$  in one facet may come from the fact that the highest-occupied and lowest-unoccupied molecular orbitals into which the hole and electron, respectively, are injected have different spatial distributions.

In case of a *standing* or a *lying*  $\pi$ -conjugated molecule or its two-dimensional array, the change or shift in energy level of the injected charge is understood based on the basic electrostatics, and it also depends on the polarity of H-C or F-C bonds.<sup>36</sup> The calculated  $S^+$  and

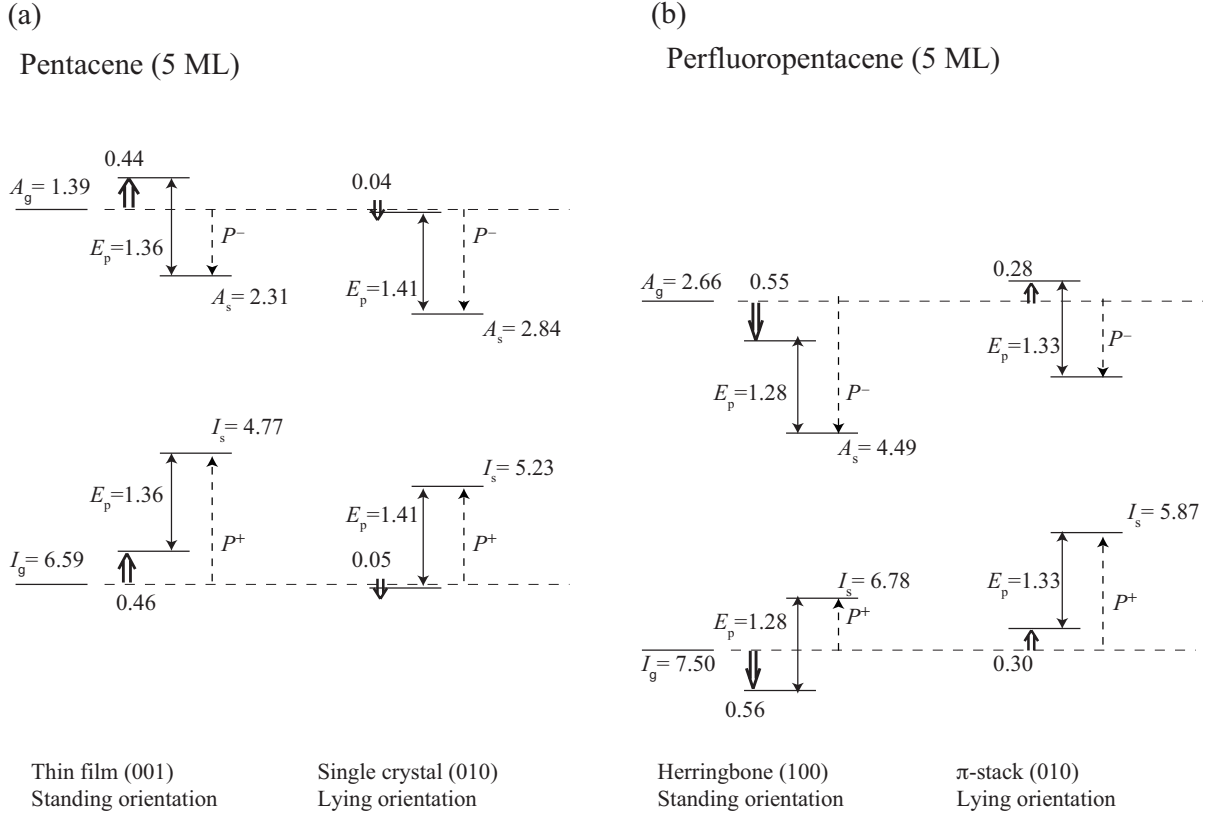


FIG. 3. Schematic of the determination of  $I_s$  and  $A_s$  for the pentacene and perfluoropentacene polymorphs. The gas phase ionization energy ( $I_g$ ) and electron affinity ( $A_s$ ) are indicated by the horizontal dashed lines, and the vertical dashed lines display the polarization energies  $P^+$  or  $P^-$ , which are comprised of the electronic polarization  $E_p$  displayed by the double-headed arrows and the electrostatic energies  $S^+$  or  $S^-$  indicated by the thick one-headed arrows.

TABLE I. Theoretical ionization energy (IE) and electron affinity (EA) of the pentacene (PEN) polymorphs at the surface. Polarization energies  $P^+$  and  $P^-$ , as a sum of the induced electronic polarization ( $E_p$ ) and electrostatic ( $S$ ) contributions are shown (see Eqs. 1-2). The quantum mechanical effect  $\Delta^+/\Delta^-$  in Eq. 1 was implicitly taken into account by taking an average of the highest occupied or the lowest unoccupied energies over  $\mathbf{k}$  sampled in the Brillouin zone. The induced electronic polarizations on the hole and the electron are assumed to be the same, i.e.  $E_p^+ = E_p^- = E_p$ . The  $S^+$  and  $S^-$  were calculated for a five monolayer slab (see Fig. 2 (a)) at the DFT-GGA level of theory. The polarization energy  $P$  and the constituent components  $E_p$  and  $S$  are defined to be positive (negative) for stabilized (unstabilized) hole or electron. For schematics of determination of  $IE_s$  and  $EA_s$ , see Fig. 3 (a). The experimental values are shown for comparison.

	$I_s$	$A_s$	$P^+$	$P^-$	$S^+$	$S^-$	$E_p$
PEN thin film (001)							
$G_0W_0$	4.77	2.31	1.82	0.92	0.46	-0.44	1.36
evGW	5.09	1.99	1.50	0.60	0.46	-0.44	1.04
Exp.	4.90 <sup>a</sup>	2.35 <sup>b</sup>	1.69 <sup>b</sup>	0.96 <sup>b</sup>	—	—	—
PEN single crystal (010)							
$G_0W_0$	5.23	2.84	1.36	1.45	-0.05	0.04	1.41
evGW	5.53	2.54	1.06	1.15	-0.05	0.04	1.11
Exp.	5.45 <sup>c</sup>	3.14 <sup>b</sup>	1.14 <sup>b</sup>	1.75 <sup>b</sup>	—	—	—

<sup>a</sup> Refs. 67–71

<sup>b</sup> Ref. 26

<sup>c</sup> Refs. 72–74

TABLE II. Theoretical ionization energy (IE) and electron affinity (EA) of the perfluoropentacene (PFP) polymorphs at the surface. The convention is the same as in Table I.

	$I_s$	$A_s$	$P^+$	$P^-$	$S^+$	$S^-$	$E_p$
PFP herringbone (100)							
$G_0W_0$	6.78	4.49	0.72	1.83	-0.56	0.55	1.28
evGW	7.13	4.14	0.37	1.48	-0.56	0.55	0.93
Exp.	6.65 <sup>a</sup>	4.12 <sup>b</sup>	0.85 <sup>b</sup>	1.46 <sup>b</sup>	—	—	—
PFP $\pi$ -stack (010)							
$G_0W_0$	5.87	3.71	1.63	1.05	0.30	-0.28	1.33
evGW	6.21	3.37	1.29	0.71	0.30	-0.28	0.99
Exp.	6.00 <sup>c</sup>	3.58 <sup>b</sup>	1.50 <sup>b</sup>	0.92 <sup>b</sup>	—	—	—

<sup>a</sup> Refs. 67 and 75

<sup>b</sup> Ref. 26

<sup>c</sup> Ref. 43

$S^-$  in this study have the same signs as and comparable in magnitude to the electrostatic energy  $W(p)$  of standing and lying PEN and PFP as estimated based on the charge redistribution of the molecule after the charge injection.<sup>28</sup> The  $I_s$  and  $A_s$  calculated with the charge redistribution<sup>28</sup> and those obtained with the charge response kernel theory<sup>77</sup> calculations<sup>26</sup> are in agreement with the present result. Given that  $E_p^+$  and  $E_p^-$  may be assumed to be the same for a hole and an electron,<sup>29</sup> difference in the calculated  $S^+$  or  $S^-$  between the different polymorphs of PFP or PEN should be similar to the difference in the  $I_s$  or  $A_s$ . Actually, the magnitude of difference in the calculated  $S^+$  ( $S^-$ ) between the *standing* and *lying* configurations becomes 0.51 eV (0.48 eV) for PEN, and 0.86 eV (0.83 eV) for PFP, in fair agreement with the experimental counterpart of 0.55 eV (0.79 eV) for PEN, and 0.65 eV (0.54 eV) for PFP.

Based on the above observations, I propose the present approach is adequate for estimating the electrostatic energy contribution to the polarization energy, taking into account the size or the thickness of an organic semiconductor thin film.

#### IV. CONCLUSIONS

The energy of the injected charge, i.e. hole and electron, at the organic semiconductor surface was theoretically investigated with the  $GW$  approximation and the periodic slab approach within DFT-GGA. While the former methodology treated the electronic polarization energy, which is isotropic and is dependent on the electronic nature of the bulk phase, the latter approach explicitly treated the electrostatic nature of the organic molecules at the surface, which is in general anisotropic and thus depends on the orientation of the molecules at the surface. The resulting ionization energies ( $I_s$ ) and electron affinities ( $A_s$ ) of pentacene (PEN) and perfluoropentacene (PFP) crystals, whose constituent molecules have the opposite polarity of constituent chemical bonds and thus their opposite principal components of the quadrupole

moment with similar magnitude, are in agreement with a body of the recent experimental results on the thin films obtained with the ultraviolet photoemission or the low-energy inverse photoemission spectroscopy techniques. As far as the electrostatic contribution  $S^+$  or  $S^-$  is concerned, the results were in fair agreement with the theoretical model results based on the charge redistribution of the molecules or those based on the charge response kernel theory, and were also in agreement with the estimation based on the experimental  $I_s$  and  $A_s$ .

Overall, while the electronic polarization  $E_p$ , approximated by the charge-induced dipole interaction, is quantitatively well described within the  $GW$  approximation, as demonstrated before, the present methodology of estimating the electrostatic contribution  $S$  as the difference in frontier orbital energies between the gas phase and the slab of the surface seems to describe well the electrostatic nature of the molecular orientation dependence of  $I_s$  and  $A_s$  at the surface, i.e., the charge-quadrupole interaction. The present first-principles method of predicting  $I_s$  and  $A_s$  is suitable for organic semiconductor nano-scale films comprised of a few monolayers, as investigated in this study. The method lacks description of the decreasing polarization at the surface which amounts to the change of the quantities by  $\approx 0.2$  eV. Nevertheless, considering the huge computational cost involved in full treatment of the slab at the  $GW$  level of theory, the method is suitable at the moment for quantitative treatment of an organic semiconductor nano-scale thin film, which is required for nano-scale or sub-nanoscale control of the materials electronic properties.

Treatment of a thin film should be taken care of, for instance, the number of monolayers required to make comparison of the theoretical result with the experimental result on equal footing. In the present case of pristine PEN and PFP, it was estimated that a thin film slab with smaller number of the monolayers or the one with its thickness of  $\approx 20$  monolayers changed the result by only 0.1 eV or smaller. However, as far as a mixed film such as the donor-acceptor heterojunctions relevant to organic photovoltaics<sup>78</sup> is concerned, tuning the number of the layers may be critical, since there is appreciable attrac-

tive electrostatic interaction within the donor-acceptor pair. A study applying the same methodology to the donor-acceptor mixed films is underway.<sup>79</sup>

### ACKNOWLEDGMENTS

The author is grateful to Alban de Gary of Université Toulouse III Paul Sabatier and Hiroyuki Yoshida of Chiba University for fruitful discussion. The author also would like to thank Yoshitada Morikawa and Iku-taro Hamada of Osaka University for providing me with pseudopotentials of a F atom used in this study. This work was partly supported by Grants-in-Aid for Scientific

Research on Innovative Areas “3D Active-Site Science” (No. 26105011), and for Fund for the Promotion of Joint International Research (Fostering Joint International Research) (No. 16KK0115) from Japan Society for the Promotion of Science (JSPS), and by “Joint Usage/Research Center for Interdisciplinary Large-scale Information Infrastructures” and “High Performance Computing Infrastructure” in Japan (Project ID: jh190062-NAH). The author acknowledges the Supercomputer Center, the Institute for Solid State Physics, the University of Tokyo, and the Cyberscience Center, Tohoku University, for the use of their facilities. The molecular graphics were generated with the VESTA<sup>80</sup> software.

- 
- \* Electronic address: shou@sci.u-ryukyu.ac.jp
- <sup>1</sup> J.-P. Yang, F. Bussolotti, S. Kera, and N. Ueno, *J. Phys. D: Appl. Phys.* **50**, 423002 (2017).
  - <sup>2</sup> K. Akaike, *Jpn. J. Appl. Phys.* **57**, 03EA03 (2018).
  - <sup>3</sup> L. Hedin, *Phys. Rev.* **139**, A796 (1965).
  - <sup>4</sup> F. Aryasetiawan and O. Gunnarsson, *Rep. Prog. Phys.* **61**, 237 (1998).
  - <sup>5</sup> C. A. Rozzi, D. Varsano, A. Marini, E. K. U. Gross, and A. Rubio, *Phys. Rev. B* **73**, 205119 (2006).
  - <sup>6</sup> S. Ismail-Beigi, *Phys. Rev. B* **73**, 233103 (2006).
  - <sup>7</sup> J. B. Neaton, M. S. Hybertsen, and S. G. Louie, *Phys. Rev. Lett.* **97**, 216405 (2006).
  - <sup>8</sup> J. M. Garcia-Lastra, C. Rostgaard, A. Rubio, and K. S. Thygesen, *Phys. Rev. B* **80**, 245427 (2009).
  - <sup>9</sup> Y. Chen, I. Tamblyn, and S. Y. Quek, *J. Phys. Chem. C* **121**, 13125 (2017).
  - <sup>10</sup> I. Tamblyn, P. Darancet, S. Y. Quek, S. A. Bonev, and J. B. Neaton, *Phys. Rev. B* **84**, 201402 (2011).
  - <sup>11</sup> V. Barone, M. Cossi, and J. Tomasi, *J. Chem. Phys.* **107**, 3210 (1997).
  - <sup>12</sup> A. Warshel and M. Levitt, *J. Mol. Biol.* **103**, 227 (1976).
  - <sup>13</sup> M. J. Field, P. A. Bash, and M. Karplus, *J. Comput. Chem.* **11**, 700 (1990).
  - <sup>14</sup> M. Svensson, S. Humbel, R. D. J. Froese, T. Matsubara, S. Sieber, and K. Morokuma, *J. Phys. Chem.* **100**, 19357 (1996).
  - <sup>15</sup> M. Svensson, S. Humbel, and K. Morokuma, *J. Chem. Phys.* **105**, 3654 (1996).
  - <sup>16</sup> J. E. Norton and J.-L. Brédas, *J. Am. Chem. Soc.* **130**, 12377 (2008).
  - <sup>17</sup> P. K. Nayak and N. Periasamy, *Org. Electron.* **10**, 1396 (2009).
  - <sup>18</sup> S. Difley, L.-P. Wang, S. Yeganeh, S. R. Yost, and T. V. Voorhis, *Acc. Chem. Res.* **43**, 995 (2010).
  - <sup>19</sup> P. Friederich, F. Symalla, V. Meded, T. Neumann, and W. Wenzel, *J. Chem. Theory Comput.* **10**, 3720 (2014).
  - <sup>20</sup> X. Blase, C. Attaccalite, and V. Olevano, *Phys. Rev. B* **83**, 115103 (2011).
  - <sup>21</sup> J. Li, G. D’Avino, I. Duchemin, D. Beljonne, and X. Blase, *J. Phys. Chem. Lett.* **7**, 2814 (2016).
  - <sup>22</sup> J. Li, G. D’Avino, I. Duchemin, D. Beljonne, and X. Blase, *Phys. Rev. B* **97**, 035108 (2018).
  - <sup>23</sup> J. P. Perdew, K. Burke, and M. Ernzerhof, *Phys. Rev. Lett.* **77**, 3865 (1996).
  - <sup>24</sup> Y. Kang, S. H. Jeon, Y. Cho, and S. Han, *Phys. Rev. B* **93**, 035131 (2016).
  - <sup>25</sup> G. D’Avino, L. Muccioli, F. Castet, C. Poelking, D. Andrienko, Z. G. Soos, J. Cornil, and D. Beljonne, *J. Phys.: Condens. Matter* **28**, 433002 (2016).
  - <sup>26</sup> H. Yoshida, K. Yamada, J. Tsutsumi, and N. Sato, *Phys. Rev. B* **92**, 075145 (2015).
  - <sup>27</sup> S. M. Ryno, C. Risko, and J.-L. Brédas, *ACS Appl. Mater. Interfaces* **8**, 14053 (2016).
  - <sup>28</sup> B. J. Topham and Z. G. Soos, *Phys. Rev. B* **84**, 165405 (2011).
  - <sup>29</sup> K. Yamada, S. Yanagisawa, T. Koganezawa, K. Mase, N. Sato, and H. Yoshida, *Phys. Rev. B* **97**, 245206 (2018).
  - <sup>30</sup> S. Yanagisawa, *AIP Conf. Proc.* **1906**, 030014 (2017).
  - <sup>31</sup> K. Seki, H. Inokuchi, and Y. Harada, *Chem. Phys. Lett.* **20**, 197 (1973).
  - <sup>32</sup> K. Seki, Y. Harada, K. Ohno, and H. Inokuchi, *Bull. Chem. Soc. Jpn.* **47**, 1608 (1974).
  - <sup>33</sup> F. Gutmann and L. E. Lyons, *Organic Semiconductors* (John Wiley and Sons, Inc., New York, Sydney, 1967).
  - <sup>34</sup> N. Sato, K. Seki, and H. Inokuchi, *J. Chem. Soc., Faraday Trans.* **2**, 1621 (1981).
  - <sup>35</sup> S. Duhm, G. Heimel, I. Salzmann, H. Glowatzki, R. L. Johnson, A. Vollmer, J. P. Rabe, and N. Koch, *Nat. Mater.* **7**, 326 EP (2008).
  - <sup>36</sup> G. Heimel, I. Salzmann, S. Duhm, and N. Koch, *Chem. Mater.* **23**, 359 (2011).
  - <sup>37</sup> Y. Morikawa, H. Ishii, and K. Seki, *Phys. Rev. B* **69**, 041403(R) (2004).
  - <sup>38</sup> T. Siegrist, C. Kloc, J. H. Schön, B. Batlogg, R. C. Haddon, S. Berg, and G. A. Thomas, *Angew. Chem. Int. Ed. Engl.* **40**, 1732 (2001).
  - <sup>39</sup> H. Yoshida, K. Inaba, and N. Sato, *Appl. Phys. Lett.* **90**, 181930 (2007).
  - <sup>40</sup> I. P. M. Bouchoms, W. A. Schoonveld, J. Vrijmoeth, and T. M. Klapwijk, *Synth. Met.* **104**, 175 (1999).
  - <sup>41</sup> W. H. Lee, J. Park, S. H. Sim, S. Lim, K. S. Kim, B. H. Hong, and K. Cho, *J. Am. Chem. Soc.* **133**, 4447 (2011).
  - <sup>42</sup> I. Salzmann, S. Duhm, G. Heimel, J. P. Rabe, N. Koch, M. Oehzelt, Y. Sakamoto, and T. Suzuki, *Langmuir* **24**, 7294 (2008).
  - <sup>43</sup> I. Salzmann, A. Moser, M. Oehzelt, T. Breuer, X. Feng, Z.-Y. Juang, D. Nabok, R. G. Della Valle, S. Duhm, G. Heimel, A. Brillante, E. Venuti, I. Bilotti,

- C. Christodoulou, J. Frisch, P. Puschnig, C. Draxl, G. Witte, K. Müllen, and N. Koch, *ACS Nano* **6**, 10874 (2012).
- <sup>44</sup> S. Grimme, *J. Comput. Chem.* **27**, 1787 (2006).
- <sup>45</sup> N. Troullier and J. L. Martins, *Phys. Rev. B* **43**, 1993 (1991).
- <sup>46</sup> M. S. Hybertsen and S. G. Louie, *Phys. Rev. B* **34**, 5390 (1986).
- <sup>47</sup> M. M. Rieger, L. Steinbeck, I. D. White, H. N. Rojas, and R. W. Godby, *Comput. Phys. Commun.* **117**, 211 (1999).
- <sup>48</sup> L. Steinbeck, A. Rubio, L. Reining, M. Torrent, I. D. White, and R. W. Godby, *Comput. Phys. Commun.* **125**, 105 (2000).
- <sup>49</sup> C. Freysoldt, P. Eggert, P. Rinke, A. Schindlmayr, R. W. Godby, and M. Scheffler, *Comput. Phys. Commun.* **176**, 1 (2007).
- <sup>50</sup> C. Faber, P. Boulanger, C. Attaccalite, I. Duchemin, and X. Blase, *Phil. Trans. R. Soc. A* **372** (2014).
- <sup>51</sup> S. Körbel, P. Boulanger, I. Duchemin, X. Blase, M. A. L. Marques, and S. Botti, *J. Chem. Theory Comput.* **10**, 3934 (2014).
- <sup>52</sup> C. Rostgaard, K. W. Jacobsen, and K. S. Thygesen, *Phys. Rev. B* **81**, 085103 (2010).
- <sup>53</sup> S. Sharifzadeh, A. Biller, L. Kronik, and J. B. Neaton, *Phys. Rev. B* **85**, 125307 (2012).
- <sup>54</sup> F. Caruso, P. Rinke, X. Ren, M. Scheffler, and A. Rubio, *Phys. Rev. B* **86**, 081102 (2012).
- <sup>55</sup> F. Bruneval and M. A. L. Marques, *J. Chem. Theory Comput.* **9**, 324 (2013).
- <sup>56</sup> M. Govoni and G. Galli, *J. Chem. Theory Comput.* **11**, 2680 (2015).
- <sup>57</sup> W. Luo, S. Ismail-Beigi, M. L. Cohen, and S. G. Louie, *Phys. Rev. B* **66**, 195215 (2002).
- <sup>58</sup> V. Coropceanu, M. Malagoli, D. A. da Silva Filho, N. E. Gruhn, T. G. Bill, and J. L. Brédas, *Phys. Rev. Lett.* **89**, 275503 (2002).
- <sup>59</sup> M. C. R. Delgado, K. R. Pigg, D. A. da Silva Filho, N. E. Gruhn, Y. Sakamoto, T. Suzuki, R. M. Osuna, J. Casado, V. Hernández, J. T. L. Navarrete, N. G. Martinelli, J. Cornil, R. S. Sánchez-Carrera, V. Coropceanu, and J.-L. Brédas, *J. Am. Chem. Soc.* **131**, 1502 (2009).
- <sup>60</sup> L. Crocker, T. Wang, and P. Kebarle, *J. Am. Chem. Soc.* **115**, 7818 (1993).
- <sup>61</sup> G. Heimel, S. Duhm, I. Salzmann, A. Gerlach, A. Strozecka, J. Niederhausen, C. Bürker, T. Hosokai, I. Fernandez-Torrente, G. Schulze, S. Winkler, A. Wilke, R. Schlesinger, J. Frisch, B. Bröker, A. Vollmer, B. Detlefs, J. Pflaum, S. Kera, K. J. Franke, N. Ueno, J. I. Pascual, F. Schreiber, and N. Koch, *Nat. Chem.* **5**, 187 (2013).
- <sup>62</sup> S. Refaely-Abramson, S. Sharifzadeh, M. Jain, R. Baer, J. B. Neaton, and L. Kronik, *Phys. Rev. B* **88**, 081204 (2013).
- <sup>63</sup> D. Vanderbilt, *Phys. Rev. B* **41**, 7892 (1990).
- <sup>64</sup> H. Yoshida and N. Sato, *Phys. Rev. B* **77**, 235205 (2008).
- <sup>65</sup> W. Kohn, *Phys. Rev. Lett.* **76**, 3168 (1996).
- <sup>66</sup> D. Deutsch, A. Natan, Y. Shapira, and L. Kronik, *J. Am. Chem. Soc.* **129**, 2989 (2007).
- <sup>67</sup> S. Duhm, I. Salzmann, G. Heimel, M. Oehzelt, A. Haase, R. L. Johnson, J. P. Rabe, and N. Koch, *Appl. Phys. Lett.* **94**, 033304 (2009).
- <sup>68</sup> Y. M. Lee, J. W. Kim, H. Min, T. G. Lee, and Y. Park, *Curr. Appl. Phys.* **11**, 1168 (2011).
- <sup>69</sup> I. Salzmann, G. Heimel, S. Duhm, M. Oehzelt, P. Pingel, B. M. George, A. Schnegg, K. Lips, R.-P. Blum, A. Vollmer, and N. Koch, *Phys. Rev. Lett.* **108**, 035502 (2012).
- <sup>70</sup> P. Sehati, S. Braun, and M. Fahlman, *Chem. Phys. Lett.* **583**, 38 (2013).
- <sup>71</sup> Y. Nakayama, Y. Uragami, M. Yamamoto, S. Machida, H. Kinjo, K. Mase, K. R. Koswattage, and H. Ishii, *Jpn. J. Appl. Phys.* **53**, 01AD03 (2013).
- <sup>72</sup> N. Koch, A. Vollmer, S. Duhm, Y. Sakamoto, and T. Suzuki, *Adv. Mater.* **19**, 112 (2007).
- <sup>73</sup> H. Yamane, K. Kanai, Y. Ouchi, N. Ueno, and K. Seki, *J. Electron Spectrosc. Relat. Phenomena* **174**, 28 (2009).
- <sup>74</sup> H. Fukagawa, H. Yamane, T. Kataoka, S. Kera, M. Nakamura, K. Kudo, and N. Ueno, *Phys. Rev. B* **73**, 245310 (2006).
- <sup>75</sup> I. Salzmann, S. Duhm, G. Heimel, M. Oehzelt, R. Kniprath, R. L. Johnson, J. P. Rabe, and N. Koch, *J. Am. Chem. Soc.* **130**, 12870 (2008).
- <sup>76</sup> T. Rangel, K. Berland, S. Sharifzadeh, F. Brown-Altwater, K. Lee, P. Hyldgaard, L. Kronik, and J. B. Neaton, *Phys. Rev. B* **93**, 115206 (2016).
- <sup>77</sup> A. Morita and S. Kato, *J. Am. Chem. Soc.* **119**, 4021 (1997).
- <sup>78</sup> M. Schwarze, K. S. Schellhammer, K. Ortstein, J. Benduhn, C. Gaul, A. Hinderhofer, L. Perdígón Toro, R. Scholz, J. Kublitski, S. Roland, M. Lau, C. Poelking, D. Andrienko, G. Cuniberti, F. Schreiber, D. Neher, K. Vandewal, F. Ortman, and K. Leo, *Nat. Commun.* **10**, 2466 (2019).
- <sup>79</sup> Y. Uemura, S. Abudullah, S. Yanagisawa, and H. Yoshida, Unsubmitted.
- <sup>80</sup> K. Momma and F. Izumi, *J. Appl. Crystallogr.* **44**, 1272 (2011).